

ChemComm

Accepted Manuscript



This is an *Accepted Manuscript*, which has been through the Royal Society of Chemistry peer review process and has been accepted for publication.

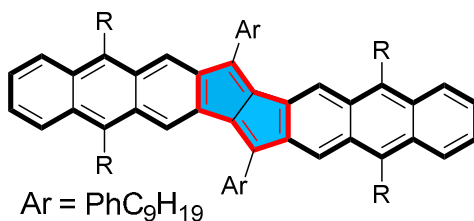
Accepted Manuscripts are published online shortly after acceptance, before technical editing, formatting and proof reading. Using this free service, authors can make their results available to the community, in citable form, before we publish the edited article. We will replace this *Accepted Manuscript* with the edited and formatted *Advance Article* as soon as it is available.

You can find more information about *Accepted Manuscripts* in the [Information for Authors](#).

Please note that technical editing may introduce minor changes to the text and/or graphics, which may alter content. The journal's standard [Terms & Conditions](#) and the [Ethical guidelines](#) still apply. In no event shall the Royal Society of Chemistry be held responsible for any errors or omissions in this *Accepted Manuscript* or any consequences arising from the use of any information it contains.

Graphical Abstract:

Two stable dianthraceno[*a,e*]pentalenes were synthesized and **DAP2** exhibited high charge carrier mobility of $0.65 \text{ cm}^2\text{V}^{-1}\text{s}^{-1}$ due to its dense packing.



Ar = PhC₉H₁₉

DAP1 R = H $\mu_{\text{h}} = 0.001 \text{ cm}^2\text{V}^{-1}\text{S}^{-1}$

DAP2 R = Ph $\mu_{\text{h}} = 0.65 \text{ cm}^2\text{V}^{-1}\text{S}^{-1}$

Cite this: DOI: 10.1039/c0xx00000x

www.rsc.org/xxxxxx

COMMUNICATION

Dianthraceno[*a,e*]pentalenes: Synthesis, Crystallographic Structures and Applications for Organic Field-Effect Transistors

Gaole Dai,^a Jingjing Chang,^a Wenhua Zhang,^b Shiqiang Bai,^b Kuo-Wei Huang,^c Jianwei Xu,^b and Chunyan Chi^{*a}

Received (in XXX, XXX) Xth XXXXXXXXXX 20XX, Accepted Xth XXXXXXXXXX 20XX

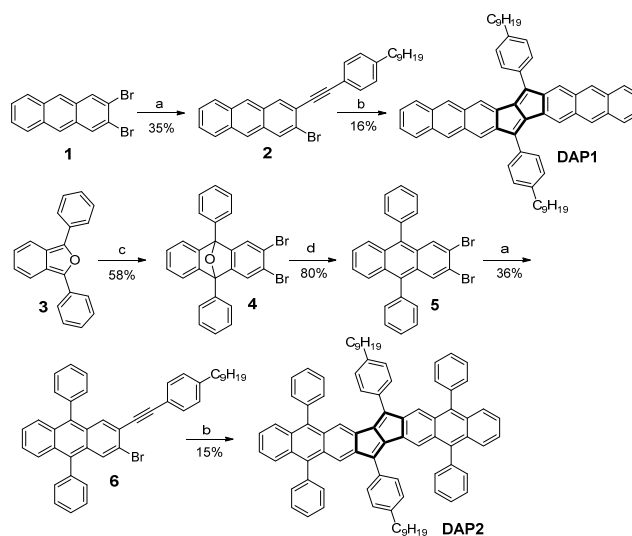
DOI: 10.1039/b000000x

Two soluble and stable dianthraceno[*a,e*]pentalenes with two (DAP1) and six (DAP2) phenyl substituents were synthesized. Both compounds possess a small energy band gap and show amphoteric redox behaviour due to intramolecular donor-accepter interactions. X-ray crystallographic analysis revealed that DAP2 showed a closely packed structure with multi-dimensional [C-H... π] interactions although there are no π - π interactions between the dianthraceno[*a,e*]pentalene cores. As a result, solution-processed field effect transistors from DAP2 exhibited an average hole mobility of $0.65 \text{ cm}^2 \text{ V}^{-1} \text{ s}^{-1}$. Under similar conditions, DAP1 showed an average field effect hole mobility of $0.001 \text{ cm}^2 \text{ V}^{-1} \text{ s}^{-1}$.

Linear π -extended acenes such as pentacene have been demonstrated to be very good charge transporting materials.¹ Higher mobilities are expected for the even longer acenes, but their intrinsic high reactivity limited their synthesis and material applications.² Incorporation of an antiaromatic pentalene³ unit into the acene framework is expected to be an efficient approach to stabilize the acene moieties due to the intramolecular donor-accepter interactions. Recently, tremendous progress has been made on synthetic methodologies for accessing stable pentalene derivatives,⁴ thus promoting research on their application for organic electronics.⁵ For example, dibenzo- and dinaphtho-fused stable pentalenes have been successfully synthesized but their applications for electronic devices are limited due to their low charge carrier mobilities.^{5a} Extension of the aceno- moieties is expected to result in superior charge transporting materials if the molecules can form ordered packing in solid state. In this work, two dianthraceno[*a,e*]pentalene derivatives (DAP1 and DAP2, Scheme 1) with two or six phenyl substituents are synthesized and their performance in organic field effect transistors (OFETs) was evaluated. It was found that the six phenyl rings substituted compound DAP2 showed the highest hole mobility (average $0.65 \text{ cm}^2 \text{ V}^{-1} \text{ s}^{-1}$) among all reported pentalene-based semiconductors, which can be correlated to its unique packing structure.

The synthesis of DAP1 and DAP2 is based on a Pd-catalyzed cyclodimerization reaction (Scheme 1).^{4d,e} Controlled Sonogashira coupling reaction between 2,3-dibromoanthracene **1**⁶ and 1-ethynyl-4-nonylbenzene⁷ gave the 2-bromo-3-((4-nonylphenyl)ethynyl)anthracene **2** in 35% yield. Subsequent Pd₂(dba)₃ catalyzed cyclodimerization of **2** afforded the 7,16-bis(4-nonylphenyl) dianthraceno[*a,e*]pentalene DAP1 in 16% yield. Diels-Alder addition reaction between 1,3-

diphenylisobenzofuran **3**⁸ and the *in situ* generated dibromobenzynes provided the 2,3-dibromo-9,10-diphenyl-9,10-dihydro-9,10-epoxyanthracene **4** in 58% yield. Then the key intermediate 2,3-dibromo-9,10-diphenylanthracene **5** was obtained in 80% yield by reductive de-oxygenation of **4** via zinc and titanium tetrachloride. Similar Sonogashira coupling followed by Pd-catalyzed cyclodimerization reaction gave the target compound 7,16-bis(4-nonylphenyl)-5,9,14,18-tetraphenyl dianthraceno[*a,e*]pentalene DAP2.



Scheme 1 Synthetic route to DAP1 and DAP2. Reagents and conditions: (a) 1-ethynyl-4-nonylbenzene, Pd(PPh₃)₂Cl₂, CuI, Et₃N/THF, 75 °C, overnight; (b) Pd₂(dba)₃, P(2-furyl)₃, Cs₂CO₃, CsF, hydroquinone, 1,4-dioxane, 135 °C, 36 h; (c) 1) 1,2,4,5-tetrabromobenzene, *n*-BuLi, toluene, -50 °C, 2) RT, overnight; (d) Zn, TiCl₄, THF, 0-70 °C, reflux overnight.

Compounds DAP1 and DAP2 both are stable in air and have good solubility in common organic solvents due to the attachment of the aliphatic chains.⁹ The electronic absorption maxima for DAP1 and DAP2 in chloroform are located at 369 and 379 nm, respectively (Fig. 1a), which can be correlated to the HOMO-2→LUMO+1 transitions (363.6 nm, oscillator strength $f = 1.2983$ for DAP1; 371.5 nm, $f = 1.1488$ for DAP2) based on the time dependent density functional theory (TD DFT) calculations (B3LYP/6-31G**) (Table S1-S3 and Figure S1-S2 in ESI†). A longer wavelength absorption band with maxima at 556 and 579 nm was also observed for DAP1 and DAP2, respectively, which are originated from HOMO→LUMO transitions (547.3 nm, $f =$

0.5057 for **DAP1**; 557.3 nm, $f = 0.5459$ for **DAP2** by TD DFT). The calculated frontier molecular orbital profiles are shown in Fig. 1c and 1d. It was found that the HOMOs of the two molecules are delocalized along the dianthraceno[*a,e*]pentalene framework while the LUMOs are mainly localized at the central pentalene unit. Compounds **DAP1** and **DAP2** showed obvious fluorescence in solution with maximum at 578 and 598 nm, respectively (Fig. 1a). The observed small Stokes shifts (549-685 cm^{-1}) indicate a rigid structure of the π -framework. The optical energy gaps were estimated to be 2.13 and 2.06 eV for **DAP1** and **DAP2**, respectively, based on the lowest energy absorption onset. The slight red shift of the absorption and emission spectra of **DAP2** in comparison to **DAP1** is due to the existence of additional four partially π -conjugated phenyl rings.

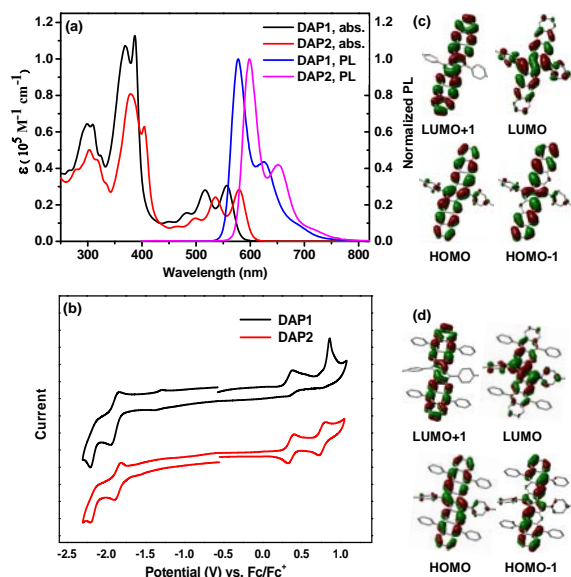


Fig. 1 (a) UV-vis absorption and photoluminescence (PL) spectra of **DAP1** and **DAP2** in chloroform; (b) Cyclic voltammograms of **DAP1** and **DAP2** recorded in dry dichloromethane; frontier molecular orbital profiles of **DAP1** (c) and **DAP2** (d) based on DFT (B3LYP/6-31G**) calculations.

Compounds **DAP1** and **DAP2** showed amphoteric redox behavior in cyclic voltammetry and differential pulse voltammetry (Fig. 1b and Fig. S3 in ESI†). Four irreversible oxidation waves with half-wave potential $E_{1/2}^{\text{ox}}$ at 0.33, 0.52, 0.74 and 0.82 V and two reversible reduction waves with half-wave potential $E_{1/2}^{\text{red}}$ at -1.94 and -2.24 V (vs. ferrocene/ferrocenium couple, Fc/Fc^+) were observed for **DAP1**. **DAP2** showed two reversible oxidation waves with $E_{1/2}^{\text{ox}}$ at 0.32 and 0.72 V, and two reversible reduction waves with $E_{1/2}^{\text{red}}$ at -1.87 and -2.20 V. The HOMO/LUMO energy levels are determined to be -5.03/-2.96 and 5.03/-3.02 for **DAP1** and **DAP2**, respectively, from the onset of the first oxidation/reduction waves (ESI†). The corresponding electrochemical energy gaps are then estimated to be 2.07 and 2.01 eV for **DAP1** and **DAP2**, which is in agreement with the optical energy gaps. The measured energy levels are also in consistency with the DFT calculations. Although the four phenyl rings attached onto the anthracene units have less influence on the electronic properties, they block the active positions and stabilize the corresponding charged species and led to better electrochemical reversibility.

Single crystals of **DAP1** and **DAP2** suitable for X-ray crystallographic analysis were obtained by slow diffusion of methanol or acetonitrile into a chloroform solution. Both

compounds have a rigid planar dianthraceno[*a,e*]pentalene framework and the two 4-nonylphenyl substituents have a torsion angle of 42-45° to the plane of pentalene (Fig. 2 and Fig. 3). The four phenyl rings in **DAP2** are almost perpendicular to the anthracene unit (dihedral angle: 84°). In **DAP1**, the two dianthraceno[*a,e*]pentalene units form a π -stacked dimer with a π - π distance of 3.367 Å and these dimers are packed into a layer like structure *via* [C-H... π] interactions (2.891 Å) between the β -H of the aliphatic chain and the core skeleton (Fig. 2). Due to the bulky substituents, there are no π - π interactions between the dianthraceno[*a,e*]pentalenes in **DAP2**. However, [C-H... π] interactions (2.776 to 2.836 Å) between the four phenyl rings and the dianthraceno[*a,e*]pentalene cores, together with the [C-H... π] (2.899 Å) and π - π interactions (3.347 Å) between the phenyl/4-nonylphenyl rings build a closely packed 3D network (Fig. 3). Bond length analysis shows that in both cases, large bond alternation in the pentalene skeleton as well as in the benzene rings is observed (Fig. S9 in ESI†), as a result of counterbalance between aromatic stabilization of the anthracene units and destabilization of the pentalene moiety.

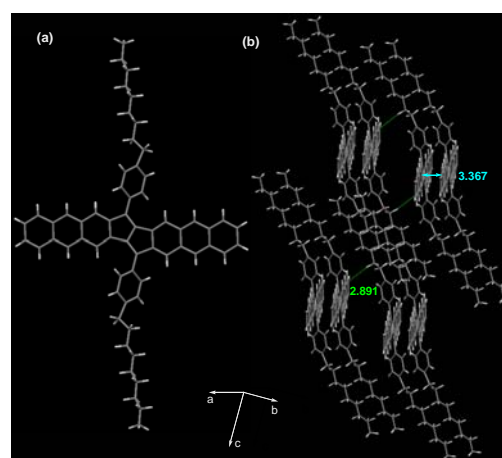


Fig. 2 (a) Crystallographic structure of **DAP1**; (b) 3D packing structure of **DAP1**, showing intermolecular π - π and [C-H... π] interactions.

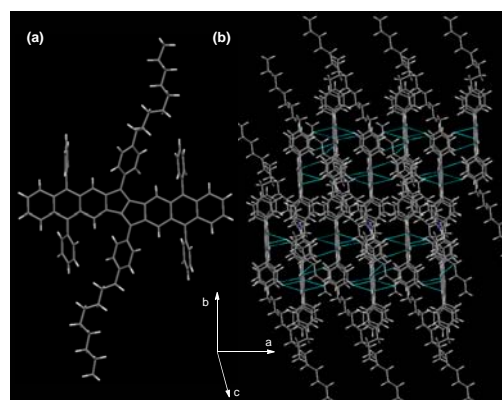


Fig. 3 (a) Crystallographic structure of **DAP2**; (b) 3D packing structure of **DAP2**, showing close contacts *via* [C-H... π] and π - π interactions.

Compounds **DAP1** and **DAP2** showed good thermal stability with decomposition temperatures at 395 and 441 °C, and displayed crystal phase below 213 and 290°C respectively (Fig. S4 in ESI†). Field effect transistors of both compounds were fabricated by solution processed thin films using a bottom-gate top-contact device structure. All devices measured in N_2 exhibited *p*-type behavior with well-defined characteristics (Fig. 4). The transfer curve revealed

an average hole mobility (μ_h) of $0.001 \text{ cm}^2\text{V}^{-1}\text{s}^{-1}$, threshold voltage (V_T) of 0 V, and current on/off ratio ($I_{\text{on}}/I_{\text{off}}$) of 10^4 for **DAP1**. However, for **DAP2**, the average μ_h value is around $0.65 \text{ cm}^2\text{V}^{-1}\text{s}^{-1}$, and the maximum mobility could reach up to $0.86 \text{ cm}^2\text{V}^{-1}\text{s}^{-1}$ (V_T : -2 V, $I_{\text{on}}/I_{\text{off}}$: 10^5). To the best of our knowledge, this is the highest mobility value for solution processed pentalene-based semiconductors. The surface morphologies and microstructures of the thin films were checked by tapping-mode atomic force microscopy (AFM) and X-ray diffraction (XRD). The thin films of **DAP1** exhibited needle-like crystals with a lot of grain boundaries (Fig. S6 in ESI†) while thin films of **DAP2** showed interconnected plate-like crystals (Fig. S7 in ESI†). The XRD pattern (Fig. S8 in ESI†) disclosed that both of the thin films showed an ordered lamellar packing structure, with the primary d-spacing of 19.97 Å and 18.02 Å for **DAP1** and **DAP2**, respectively. Therefore, the higher mobility of **DAP2** compared to **DAP1** could be explained by its more closely packed structure in solid state as well as good thin film morphology.

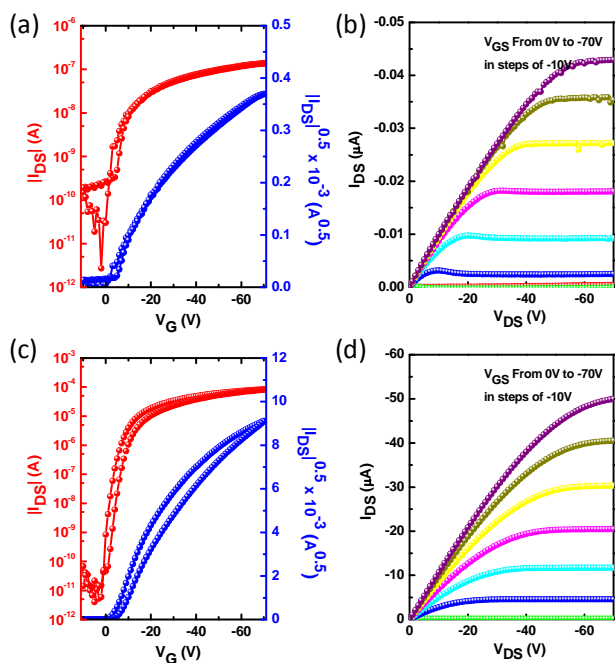


Fig. 4 Transfer and output characteristics of **DAP1** (a, b) and **DAP2** (c, d) devices with ODTS treatment.

In summary, two dianthraceno[*a,e*]pentalene derivatives **DAP1** and **DAP2** were synthesized, which represent the longest acene fused pentalene derivatives reported so far. Both compounds are stable and showed amphoteric redox behavior due to intramolecular donor-acceptor interaction. X-ray crystallographic analysis revealed a densely packed structure for **DAP2** mainly via close [C-H... π] interactions. As a result, high FET mobility was achieved for solution processed thin films of **DAP2**. Our research also demonstrated that continuous π - π stacking is not the prerequisite for efficient charge transport.

This work was financially supported from NUS Start-Up Grant (R-143-000-486-133) and MOE AcRF grants (R-143-000-510-112 and R-143-000-573-112) (C.C.), NUS-IMRE Molecular Material Center (J.X.), and KAUST (K.W.H.).

Notes and references

- ^a Department of Chemistry, National University of Singapore, 3 Science Drive 3, 117543, Singapore. Fax: +65 6779 1691; Tel: +65 6516 5375; E-mail: chmcc@nus.edu.sg
- ^b Institute of Materials Research and Engineering, A*Star, 3 Research Link, Singapore 117602.
- ^c Division of Physical Science and Engineering and KAUST Catalysis Center, King Abdullah University of Science and Technology (KAUST), Thuwal 23955-6900, Kingdom of Saudi Arabia.
- [†] Electronic Supplementary Information (ESI) available: Synthetic procedures and characterization data for all new compounds. DFT calculation details. Thermogravimetric analysis data. Device fabrication and characterization details. CCDC 1008483, 1008484. X-ray crystallographic data. See DOI: 10.1039/b000000x/
- (a) M. Bendikov, F. Wudl and D. F. Perepichka, *Chem. Rev.*, 2004, **104**, 4891; (b) J. E. Anthony, *Angew. Chem. Int. Ed.*, 2008, **47**, 452; (c) Q. Ye, C. Chi, *Chem. Mater.* 2014, **26**, 4046.
- (a) M. M. Payne, S. R. Parkin and J. E. Anthony, *J. Am. Chem. Soc.*, 2005, **127**, 8028; (b) D. Chun, Y. Cheng and F. Wudl, *Angew. Chem. Int. Ed.*, 2008, **47**, 8380; (c) R. Mondal, C. Tonshoff, D. Khon, D. C. Neckers and H. F. Bettinger, *J. Am. Chem. Soc.*, 2009, **131**, 1428; (d) I. Kaur, N. N. Stein, R. P. Kopreski and G. P. Miller, *J. Am. Chem. Soc.*, 2009, **131**, 3424; (e) I. Kaur, M. N. Jazdzzyk, N. Stein, P. Prusevich and G. P. Miller, *J. Am. Chem. Soc.* 2010, **132**, 1261; (f) H. Qu and C. Chi, *Org. Lett.*, 2010, **12**, 3360; (g) B. Purushothaman, M. Bruzek, S. R. Parkin, A. F. Miller and J. E. Anthony, *Angew. Chem. Int. Ed.* 2011, **50**, 7013; (h) M. Watanabe, Y. J. Chang, S.-W. Liu, T.-H. Chao, K. Goto, M. M. Islam, C.-H. Yuan, Y.-T. Tao, T. Shinmyozu and T. J. Chow, *Nat. Chem.*, 2012, **4**, 574; (i) H. Qu, C. Chi, *Curr. Org. Chem.* 2010, **14**, 2070.
- (a) K. Brand, *Ber. Deutsch. Chem. Ges.*, 1912, **45**, 3071; (b) H. Hopf, *Angew. Chem. Int. Ed.*, 2013, **52**, 12224.
- (a) W. C. Lothrop, *J. Am. Chem. Soc.*, 1941, **63**, 1187; (b) M. Chakraborty, C. A. Tessier and W. J. Youngs, *J. Org. Chem.*, 1999, **64**, 2947; (c) M. Saito, M. Nakamura and T. Tajima, *Chem. Eur. J.*, 2008, **14**, 6062; (d) T. Kawase, A. Konishi, Y. Hirao, K. Matsumoto, H. Kurata, T. Kubo, *Chem. Eur. J.*, 2009, **15**, 2653; (e) Z. U. Levi and T. D. Tilley, *J. Am. Chem. Soc.*, 2009, **131**, 2796; (f) H. Zhang, T. Karasawa, H. Amada, A. Wakamiya and S. Yamaguchi, *Org. Lett.*, 2009, **11**, 3076; (g) Z. U. Levi and T. D. Tilley, *J. Am. Chem. Soc.*, 2010, **132**, 11012; (h) P. Rivera-Fuentes, M. V. W. Rekowski, W. B. Schweizer, J.-P. Gisselbrecht, C. Boudon and F. Diederich, *Org. Lett.*, 2012, **14**, 4066; (i) T. Maekawa, Y. Segawa and K. Itami, *Chem. Sci.*, 2013, **4**, 2369; (j) H. Li, B. Wei, L. Xu, W.-X. Zhang and Z. Xi, *Angew. Chem. Int. Ed.*, 2013, **52**, 10822; (k) C. Chen, M. Harhausen, R. Liedtke, K. Bussmann, A. Fukazawa, S. Yamaguchi, J. L. Petersen, C. D. Daniliuc, R. Fröhlich, G. Kehr and G. Erker, *Angew. Chem. Int. Ed.*, 2013, **52**, 5992; (l) J. Zhao, K. Oniwa, N. Asao, Y. Yamamoto and T. Jin, *J. Am. Chem. Soc.*, 2013, **135**, 10222. (m) J. Shen, D. Yuan, Y. Qiao, X. Shen, Z. Zhang, Y. Zhong, Y. Yi and X. Zhu, *Org. Lett.*, 2014, **16**, 4924.
- (a) T. Kawase, T. Fujiwara, C. Kitamura, A. Konishi, Y. Hirao, K. Matsumoto, H. Kurata, T. Kubo, S. Shinamura, H. Mori, E. Miyazaki and K. Takimiya, *Angew. Chem. Int. Ed.*, 2010, **49**, 7728; (b) A. Konishi, T. Fujiwara, N. Ogawa, Y. Hirao, K. Matsumoto, H. Kurata, T. Kubo, C. Kitamura and T. Kawase, *Chem. Lett.*, 2010, **39**, 300; (c) X. Yin, Y. Li, Y. Zhu, Y. Kan, Y. Li and D. Zhu, *Org. Lett.*, 2011, **13**, 1520; (d) M. Nakano, I. Osaka, K. Takimiya, and T. Koganezawa, *J. Mater. Chem. C*, 2014, **2**, 64.
- M. Akula, *Org. Prep. Proced. Int.*, 1990, **22**, 102.
- (a) O. Ongayi, M. G. H. Vicente, B. Ghosh, F. R. Fronczek and K. M. Smith, *Tetrahedron*, 2010, **66**, 63; (b) P. Sista, H. Nguyen, J. W. Murphy, J. Hao, D. K. Dei, K. Palaniappan, J. Servello, R. S. Kularatne, B. E. Gnade, B. Xue, P. C. Dastoor, M. C. Biewer and M. C. Stefan, *Macromolecules*, 2010, **43**, 8063.
- F. Benderradji, M. Nechab, C. Einhorn and J. Einhorn, *Synlett*, 2006, **13**, 2035.
- Analog of **DAP1** without the nonyl chains was also prepared by similar method by it has very poor solubility.